ISSN 0031-918X, Physics of Metals and Metallography, 2017, Vol. 118, No. 7, pp. 644–651. © Pleiades Publishing, Ltd., 2017.
Original Russian Text © V.V. Balashev, V.A. Vikulov, A.A. Dimitriev, T.A. Pisarenko, E.V. Pustovalov, V.V. Korobtsov, 2017, published in Fizika Metallov i Metallovedenie, 2017, Vol. 118, No. 7, pp. 679–685.

ELECTRICAL AND MAGNETIC PROPERTIES

Evolution of the Structural and Magnetotransport Properties of Magnetite Films Depending on the Temperature of Their Synthesis on the SiO_2/Si(001) Surface

V. V. Balashev[a, b, *], V. A. Vikulov[a], A. A. Dimitriev[a, b], T. A. Pisarenko[a, b], E. V. Pustovalov[b], and V. V. Korobtsov[a, b]

[a] *Institute of the Automation and Control Processes, Far-East Branch, Russian Academy of Sciences, ul. Radio 5, Vladivostok, 690041 Russia*

[b] *School of Natural Sciences, Far-Eastern Federal University, ul. Sukhanova 8, Vladivostok, 690950 Russia*

**e-mail: balashev@mail.dvo.ru*

Received July 11, 2016; in final form, October 26, 2016

Abstract—The methods of transmission and reflection electron diffraction have been used to investigate the structure of Fe_3O_4 films depending on the temperature of their synthesis on an Si substrate coated with an ultrathin layer of SiO_2. The thus-grown polycrystalline films of magnetite had a texture, the axis of which was perpendicular to the surface of the SiO_2 film. It has been revealed that, with an increase in the growth temperature, a structural rearrangement occurs which is characterized by an increase in the volume fraction of grains with the preferred (311) orientation. A study of the magnetotransport properties of the films has shown that the magnitude of their magnetoresistance increases with an increase in the temperature of their synthesis. It has been established that in the $Fe_3O_4/SiO_2/Si$ system with a tunneling-thin layer of SiO_2 the magnetoresistance decreases as a result of the flow of an electric current through the silicon substrate.

Keywords: magnetite, texture, reflection high-energy electron diffraction (RHEED), magnetoresistance

DOI: 10.1134/S0031918X17050027

1. INTRODUCTION

Due to the complete spin polarization of electrons [1] and high Curie temperature (~580°C), magnetite (Fe_3O_4) is a promising material for some new directions of contemporary electronics, e.g., spintronics [2, 3]. The study of the magnetic and electrical properties of Fe_3O_4 films grown on different substrates is therefore now of enhanced interest. It has been shown that the films of magnetite can grow epitaxially on some substrates, e.g., α-Al_2O_3, GaAs, and MgO [4–7], or have a polycrystalline structure when grown on Si, SiO_2, and GaAs substrates [8–12]. The growth of Fe_3O_4 films on silicon substrates is of interest from the viewpoint of the formation of a heterostructure of the ferromagnet/semiconductor type with the possibility of injecting spin-polarized electrons into the semiconductor [3]. The Fe_3O_4 films grown on a clean Si surface and on a Si surface coated with a SiO_2 layer have a polycrystalline structure, which is independent of the method of the deposition of the film (pulsed laser deposition (PLD), magnetron sputtering, etc.) and of the growth conditions. On the other hand, these films can be characterized by both the complete misorientation of grains in them [13, 14] and the preferred crystallographic orientation of grains [15–18], i.e., they can have a texture.

An analysis of the literature data shows that the preferred orientation of grains in the films with a texture can depend on the experimental growth conditions. Thus, in the case of PLD [8, 19], a (111) texture was observed regardless of the type of substrate. On the other hand, in [19], it was revealed that, with a decrease in the growth temperature to 150°C, in the films with the (111) texture the appearance of grains with a (311) orientation is observed. Frequently, the study of magnetic and electrical properties is carried out depending on the thickness of the grown films of Fe_3O_4 or on the phase composition of the films of the iron oxide, which changes depending on the experimental conditions of the synthesis of films. At the same time, the data on the influence of the structural-morphological properties of the Fe_3O_4 films on the magnetotransport properties are nearly absent. In [17, 20], it was found that, in the textured film of Fe_3O_4 grown on an oxidized surface of Si by both magnetron sputtering [17] and reactive deposition of Fe in the oxygen atmosphere [20], the orientation of grains can change depending on the growth conditions. The authors of [17] have established that the change in the

structure leads to a change in the magnetic and transport properties of the film.

In our previous work [21], based on an analysis of the Raman spectroscopy data and magnetic measurements, it was shown that an increase in the temperature of the synthesis of the textured films of Fe_3O_4 leads to a structural ordering and to an increase in the effective magnetization as a result of a decrease of the amount of defects in the bulk of the film. In this work, for a detailed study of the evolution of the structural ordering, we performed an analysis of both the high-energy electron diffraction patterns and the data obtained by transmission electron microscopy. Furthermore, we investigated the magnetotransport properties of films depending on the temperature of their synthesis.

2. EXPERIMENTAL

The experiments were carried out using a Katun' ultra-high-vacuum setup equipped with systems for studying reflection high-energy electron diffraction (RHEED) and for spectral ellipsometry. The base pressure did not exceed 10^{-10} Torr. The accelerating voltage of the electron beam in the RHEED method was 20 kV; the angle of incidence of the beam onto the surface of the substrate did not exceed 1°. As the substrates, single-crystal plates of silicon (20 × 10 × 0.5 mm) of the *n* type (7.5 Ohm × cm) with a (001) orientation were used. Prior to the loading into the vacuum chamber, the surface of the samples was cleaned using a wet chemical treatment [22]. At the final stage of cleaning, on the surface of the Si substrate there was formed an ultrathin layer of SiO_2 by the treatment in a nitric acid solution (68% HNO3) at 121°C for 10 min. According to the ellipsometry data and to the results obtained in [23], the thickness of an SiO_2 layer obtained by this method is ~1.5 nm. After the sample was loaded into the vacuum chamber, it was annealed at 500°C for 1 h. The deposition of Fe onto the SiO_2/Si(001) surface was carried out by the thermal evaporation of Fe from a Knudsen cell with a crucible made of alumina (Al_2O_3). In the process of the growth of the Fe_3O_4 film on the SiO_2/Si(001) surface, the rate of deposition of Fe was ~1.2 nm/min, and the pressure of O_2 in the vacuum chamber was maintained at a level of ~1.3 × 10^{-6} Torr. The thickness of the Fe_3O_4 films grown at temperatures of 200–400°C was 100 nm.

The electron-microscopic examination was carried out using a Zeiss Libra 200 HR FE transmission electron microscope at an accelerating voltage of 200 kV. The experiments on the obtaining of the electron diffraction patterns were carried out using the selected-area electron diffraction (SAED) method by studying regions with a size of 200–500 nm.

For the investigation of the magnetotransport properties of the films obtained at different temperatures, we measured their conductivity depending on the applied external magnetic field. The measurements were conducted at room temperature (RT) on samples with a size of 10 × 5 mm by the standard four-probe method at a constant direct current $j = 1$ μA using a Keithley-2400 SourceMeter. The probing electrodes with a diameter of 0.2 mm were formed on the surface of the Fe_3O_4 film by thermal evaporation of Al through a metallic mask and were located collinearly with a step of 1 mm. The magnetic field was applied along the plane of the film; its value was varied in the range of –0.4 to +0.4 T.

3. RESULTS AND DISCUSSION

3.1. Structural Analysis of Fe_3O_4 Films

Figure 1 shows electron diffraction patterns obtained by the RHEED method and by electron microscopy on the magnetite films grown on an SiO_2/Si(001) surface at temperatures of 200 and 400°C. These patterns exhibit Debye diffraction rings that are characteristic of the polycrystalline films of Fe_3O_4 just as of those obtained in the case of transmission diffraction from the films grown without heating the substrate [12]. At the same time, it can be clearly seen that there is a qualitative distinction in the type of the intensity distribution along the rings in the case of RHEED and electron microscopy.

The RHEED patterns in Figs. 1a and 1b were obtained with an angle of incidence of the electron beam onto the plane of the surface close to 0°. Since the growth of grains of a polycrystalline film occurs along the direction of normal (**n**) to the surface [24] (Fig. 2a), the angle between the direction of the wave vector of the incident beam ($\mathbf{k}_0$) and the growth direction of grains is close to 90°. The transmission electron diffraction in the case of RHEED can only appear in the presence of a roughness formed by grains of Fe_3O_4 protruding above the surface of the film. On the other hand, in the case of electron microscopy (Fig. 2a), the wave vector of the incident beam $\mathbf{k}_0$ is directed along the normal (**n**) to the surface (along the grain-growth direction), and the diffraction pattern is registered on the reverse side of the Si(001) substrate. In this case, the diffraction of electrons takes place inside the entire volume of the Fe_3O_4 grains rather than only from their near-surface region.

Since the lateral dimensions of grains are approximately four to five times greater [21] than the average heights of the surface roughness, the sharpness of the rings obtained by using electron microscopy (Figs. 1c, 1d) is larger than the rings in the case of RHEED (Figs. 1a, 1b). Furthermore, in the diffraction patterns, localized diffraction spots can be seen in the rings, which is connected with the effect of refraction on the grains that are faceted and, as a result, have a more perfect structure [25]. In the region selected for studying the diffraction there are present grains of larger sizes, which increases the intensity and the locality of separate diffraction reflections in the ring.

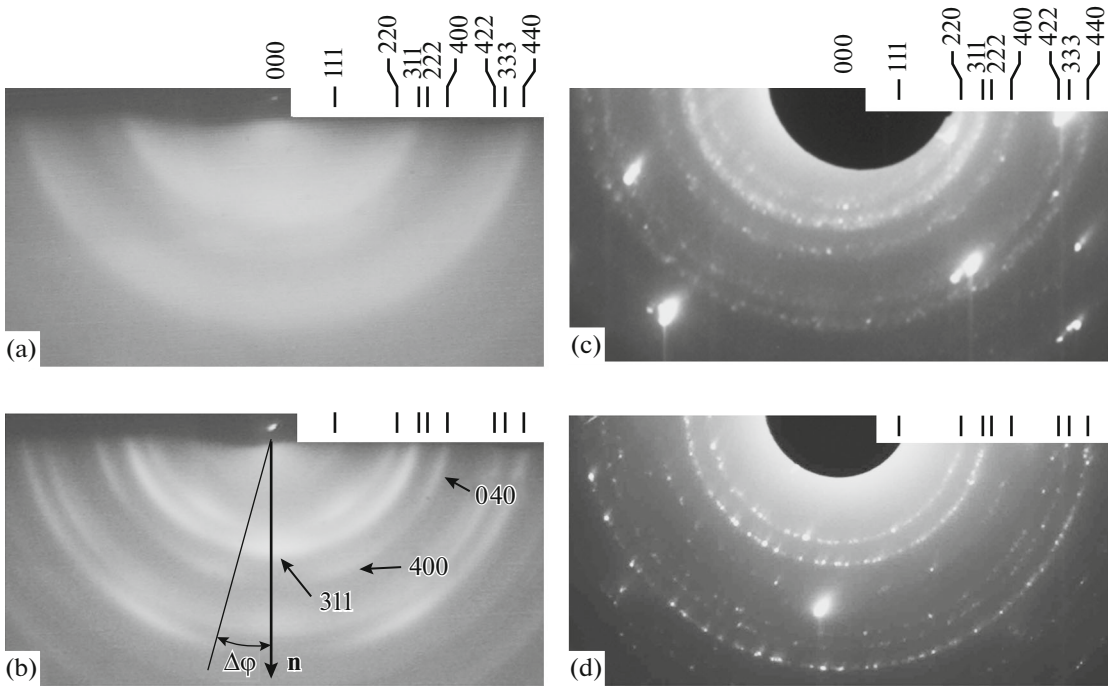

Fig. 1. Electron diffraction patterns from an Fe_3O_4 film obtained (a, b) by the RHEED method and (c, d) by the TEM. Diffraction patterns (a) and (c) correspond to the film grown at 200°C, while those shown in (b) and (d) correspond to the film grown at 400°C.

On the whole, in the region chosen for analyzing the structure (200–500 nm), the diffraction pattern does not show any preferred orientation of grains; the intensity of the diffraction rings on the average is uniform. It has been revealed that an increase in the growth temperature to 400°C leads to an increase in both the sharpness of the rings and the brightness of point reflections. This fact can be directly connected with the growth of coarse grains with a pronounced faceting.

It can be seen from Figs. 1a and 1b that the Debye rings in the case of the RHEED are characterized by a nonuniform distribution of intensity, which manifests itself in the presence of arcs. As was shown in our previous work [26], the symmetrical location of the arcs relative to the normal agrees with the theoretical diffraction pattern for the film with a (311) texture, the axis of which coincides with the normal to the surface of the film. In the case of this texture, the grains of the film are oriented so that the direction [311] of their crystal lattice is arranged preferentially along the normal (Fig. 2b). The axis of the texture in this case coincides with the normal to the surface. Since the grains have random orientation relative to the axis of the texture, the (*hkl*) nodes of the reciprocal lattice will be arranged along the rings. As can be seen from Fig. 2b, based on the example of the lattice nodes (111), (220), and (400), the deviation of the direction [311] from the axis of the texture within the limits of a certain angle ($\pm\Delta\phi$) will lead to a broadening of the rings by an angle of $2\Delta\phi$. In the case of the RHEED, the Ewald sphere, which passes along the axis of the texture (perpendicularly to the vector $\mathbf{k}_0$), intersects these rings. The points of the intersection of the rings with the Ewald sphere determine the directions of the vectors of the scattered waves. This leads to the appearance in the RHEED pattern of diffraction arcs (111), (220), (400), etc., located symmetrically relative to the axis of the texture (normal **n** to the surface), as can be seen from Figs. 1a and 1b. The angular position ($\Delta\phi$) of these arcs relative to the normal should be 29.5°, 31.5°, and 25.2°. Since, in the case of the (311) texture, the direction [311] is located preferentially along the normal to the surface, the corresponding (311) arc also is located on the normal ($\Delta\phi = 0$). It should be noted that, in the cubic lattice of grains, there are also nodes with the indices $(3\,\bar{1}\,1)$, $(3\,\bar{1}\,\bar{1})$, and $(1\,3\,\bar{1})$, the angular position of which relative to the direction (311) is ~35°, 50°, and 63°. The corresponding arcs are arranged in the RHEED pattern (Figs. 1a and 1b) symmetrically relative to the (311) arc. As can be seen from Figs. 1a and 1b, the (311), $(3\,\bar{1}\,1)$, $(3\,\bar{1}\,\bar{1})$, and $(1\,3\,\bar{1})$ arcs on the whole form a (311) ring that is almost continuous in intensity.

In the case of the TEM, the absence of arcs and a uniform distribution of the intensity in the Debye rings are explained by two reasons, namely, first, by the electron diffraction in Fe_3O_4 grains with random orientations, which are present in the lower layer of the film in the case of the competitive mode of growth

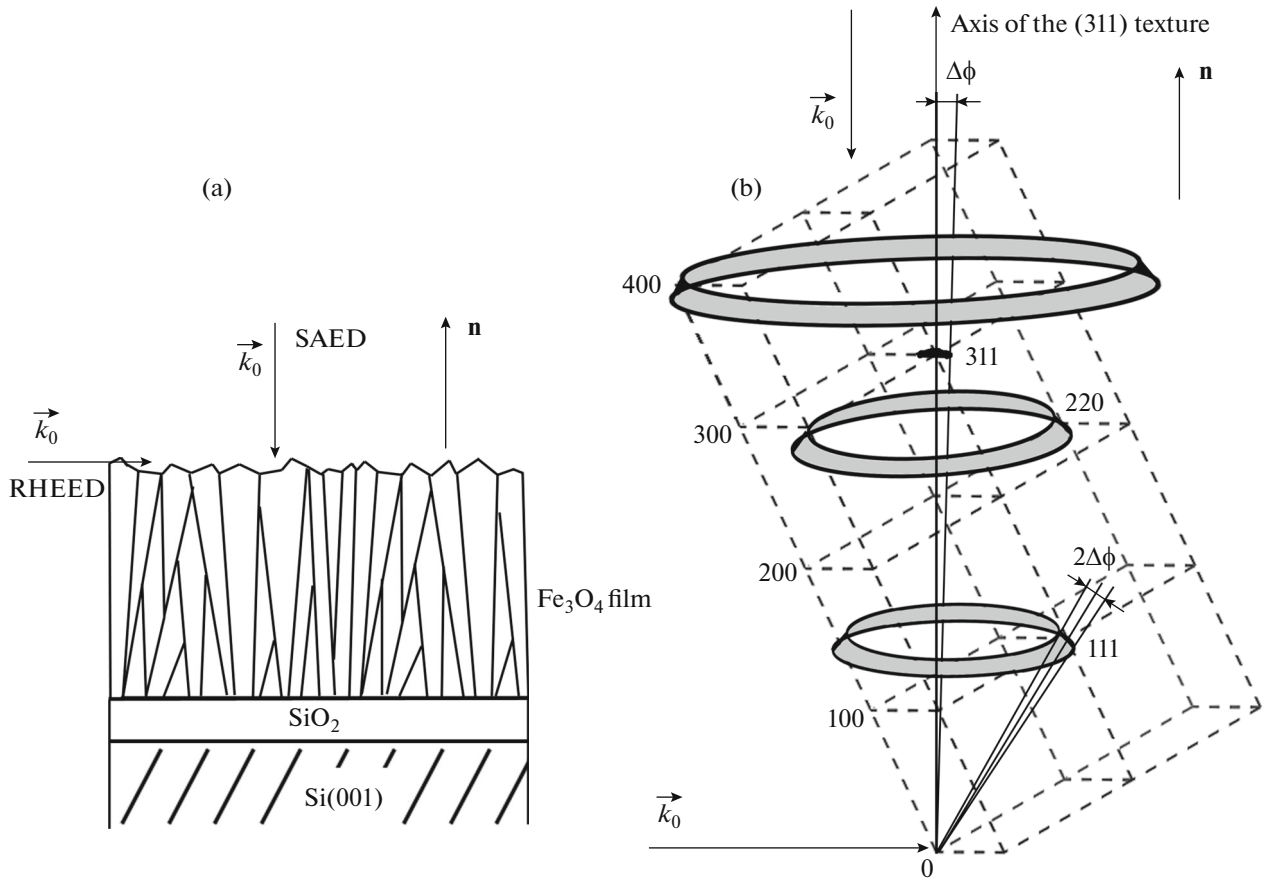

Fig. 2. (a) Schematic representation of the direction of the wave vector $\mathbf{k}_0$ of the incident electron beam relative to the Fe_3O_4 film in the case of the diffraction of high-energy electrons (RHEED) and transmission electron diffraction from a selected area of the film (SAED). (b) Orientation of the reciprocal lattice in the case of the ideal (311) texture when the axis of the texture and the [311] direction coincide.

[24]; and, second, by the geometry of diffraction, in which the vector $\mathbf{k}_0$ coincides with the axis of the texture (Fig. 2b) characteristic of the upper layer of the film. In this case, according to [25], continuous rings should also be observed with the only exception that some of them must be absent. Since the texture in the upper layer of the film is not ideal ($\Delta\phi \neq 0$) and since the grains of the lower layer have random orientations, the complete disappearance of any rings should not be observed. Since the appearance of distinct arcs in the RHEED patterns was observed only after the deposition of a film 25–30 nm thick, it can be assumed that the thickness of the lower layer with random orientations of grains does not exceed these thicknesses.

To obtain quantitative information on the effect of the temperature of growth of the Fe_3O_4 film on the texture or degree of ordering of grains in the film, we carried out measurements of the relative changes in the intensity of the arcs and of their positions relative to the normal. To this end, we carried out measurements of the angular distribution of the intensity of the (311) and (400) rings in the RHEED patterns obtained at 200°C (Fig. 1a) and 300 and 400°C (Fig. 1b). Figure 3 illustrates the corresponding angular distributions of the intensity of the (311) and (400) rings. The normalization of the intensity of the rings was performed using the procedure suggested in [27]. The dashed lines show the theoretical positions of the arcs relative to the normal to the surface for the (311) texture. As was said above, the diffraction ring (311) must include the $(3\,\bar{1}1)$, $(3\,\bar{1}\,\bar{1})$, and $(13\,\bar{1})$ arcs for which $\Delta\phi$ is equal to 0°, ±35°, ±50°, and ±63° (Fig. 3a). Since the [400] and [040] axes of the magnetite lattice are arranged at the angles of ~±25° and ±72° relative to the [311] axis, arcs from the appropriate lattice nodes should be observed in the diffraction pattern (Fig. 3b).

After the deposition at 200°C, as can be seen from Fig. 3a, the intensity of the (311) ring is almost independent of the angle ϕ. On the contrary, in the case of the (400) ring (Fig. 3b) there is observed an insignificant peak for $\Delta\phi = 0$. When the Fe_3O_4 film grows at 300°C, at $\Delta\phi = 0°$ there appears an intense peak corresponding to the (311) arc (Fig. 3a). At this growth temperature, the intensity curve for the (400) ring

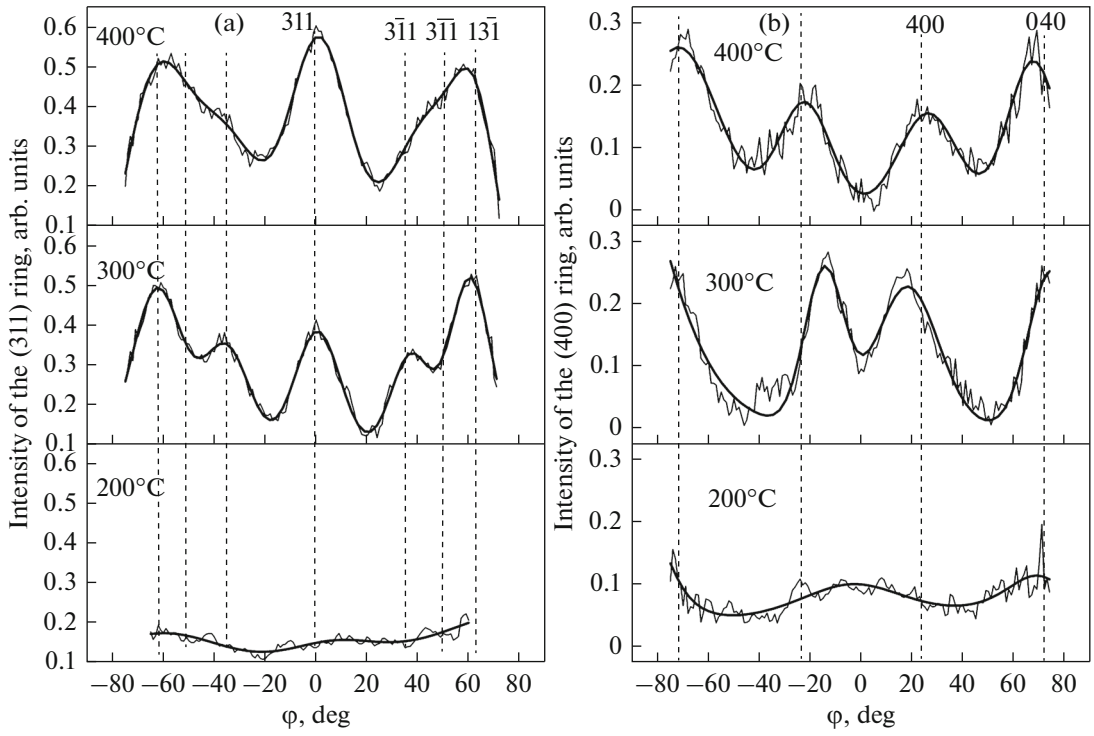

Fig. 3. Distribution of the intensity of the Debye rings (a) (311) and (b) (400) relative to the normal to the surface ($\varphi = 0°$) for the Fe_3O_4 films obtained at different growth temperatures. Position of the dashed lines corresponds to the angular position of arcs in the rings in the case of the (311) texture.

(Fig. 3b) is characterized by the appearance of two symmetrical peaks located at the angles of approximately ±16° relative to the normal to the surface. These values of the angles are approximately 9° less than the theoretical values of the location of the (400) arcs in the case of the (311) texture. The positions of the peaks that correspond to the (400) arcs reach the theoretical values of ±25° only when the growth temperature increases to 400°C. This is accompanied by an increase in the intensity of the (311) peak by almost 1.5 times compared with its value at 300°C. It was established that the width of this peak ($2\Delta\phi$) is ~30° at the growth temperatures of both 300 and 400°C. This indicates that the growth temperature does not influence the misorientation of grains relative to the axis of the texture (normal to the surface) and the angular deviation $\Delta\phi$ of the direction [311] from the axis of the texture is ~15°.

We assume that, with an increase in the temperature of growth of the Fe_3O_4 film, the volume fraction of the grains that have the orientation (311) increases, which is accompanied by both an increase in the intensity of the (311) arcs at $\Delta\phi = 0°$ and the displacements of the (400) arcs toward the appropriate theoretical positions. Thus, at 400°C (Fig. 3b), the grains in the film predominantly have (311) orientations, and the (400) and (040) reflections/arcs of the lattice are located at angles of approximately ±25° and ±72°, respectively, relative to the axis of the texture (normal to the surface). This conclusion is indirectly confirmed by a significant decrease in the intensity of the (400) ring in the case of electron microscopy (Fig. 1d). Since the Ewald sphere intersects the axis of the texture at an angle of 90°, no lattice reflections (400) and (040) located at the angles of ±25° and ±72° should occur.

In the case of the film growth at 300°C (Fig. 3b), the deviation of the lattice reflections (400) and (040) relative to their theoretical positions is ascribed to the presence of a fraction of grains that have the lattice axis [100] (rather than [311]), which is also directed along the normal to the surface. Thus, in the case of the (100) orientations of these grains, the lattice sites (400) and (040) must be arranged at an angle $\Delta\phi = 0°$ and ±90°. It can be assumed that, because of a superposition of the (400) arcs located at $\Delta\phi = 0°$ at the (100) orientation and at $\Delta\phi = 25°$ at the (311) orientation of grains, the arcs observed in the diffraction pattern are located at $\Delta\phi = 16°$.

At a temperature of 200°C (Fig. 3b), the (400) arc manifests itself in the form of a weak wide peak at $\Delta\phi = 0°$. This position of the peak can be connected with the fact that the fraction of grains that have a preferred (100) orientation becomes larger than at the temperature of 300°C. The growth of an Fe_3O_4 film with only a (100) texture was observed earlier [26] in

the case of the oxidation of a preliminarily deposited Fe film. The appearance of a (100) texture in the Fe_3O_4 film was explained by the oxidation of Fe grains with a (110) orientation. In this work, we connect the presence of the (100) orientation in a certain part of grains with the change in the mechanism of the growth of the Fe_3O_4 film at a low temperature.

3.2. Magnetotransport Properties of Fe_3O_4 Films Grown on a 1.5 nm SiO_2/Si(001) Substrate

Figure 4 shows the dependence of the magnetoresistance ($MR = (\rho_H - \rho_0)/\rho_0$) on the value of the applied magnetic field H for Fe_3O_4 films grown at different temperatures of a silicon substrate with thin (1.5 nm) and thick (1.2 μm) SiO_2 layers. It can be seen from the figure that the evolution of the MR indicates a decrease in the resistivity ρ_H of the films with an increase in the magnetic field H compared with the value of ρ_0 at $H = 0$.

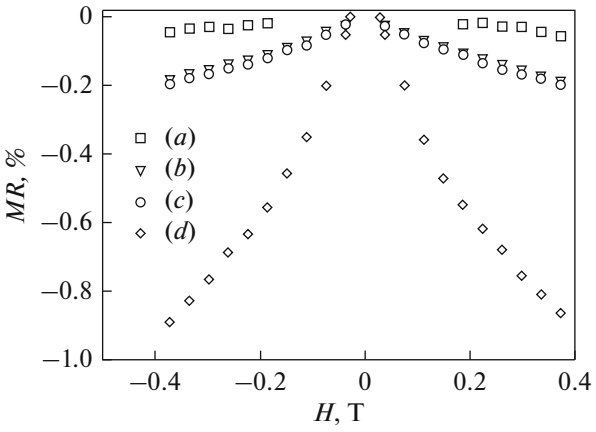

Fig. 4. Dependence of the magnetoresistance of the Fe_3O_4 films grown on the surface of a 1.5-nm SiO_2/Si(001) at various substrate temperatures: (*a*) 250°C; (*b*) 300°C; and (*c*) 400°C. Curve (*d*) was obtained for an Fe_3O_4 film grown on the surface of an SiO_2 film 1.2 μm thick at 300°C.

From a comparison of curves (*a*), (*b*), and (*c*) in Fig. 4, it can be seen that the higher the temperature of the synthesis of the films, the greater the magnitude of the *MR*. We think that an increase in the temperature of the synthesis leads not only to the growth of Fe_3O_4 grains with a preferred (311) orientation, but also to a qualitative change in the morphology of interfaces between the grains. In [13, 28], the small values of the *MR* of the Fe_3O_4 films are explained by the presence of an amorphous phase and by the violation of the stoichiometry at the grain boundaries. It was found in [29] that in the Fe_3O_4 film grown at room temperature, the interface between the grains can represent both extended disordered (amorphous) regions and regions disordered on the atomic scale. The extended disordered regions were dominant and separated the grains from each other to a distance of ~4 nm. These regions are responsible for spin disordering and strong antiferromagnetic interaction at the grain boundaries, which leads to a decrease in both the magnetization of the Fe_3O_4 films and in the spin-polarized current between the grains. We think that the small values of the *MR* of the film grown at 250°C (Fig. 4, curve (*a*)) are explained by a weak change in the transport of the spin-polarized electrons through the regions with the strong antiferromagnetic interaction. On the contrary, an increase in the *MR* of the films grown at 300 and 400°C (Fig. 4, curves (*b*) and (*c*)) can be connected with a decrease in the antiferromagnetic interaction at grain boundaries. As a result of an increase in the growth temperature, as well as in the diffusion mobility of Fe atoms and of O_2 molecules at the growth surface, the formation of the amorphous phase between the Fe_3O_4 grains should be decreased. In these films, the basic type of defects at the grain boundaries can be regions disordered on the atomic scale, which are characterized by a lower antiferromagnetic interaction. In all likelihood, this is responsible for both an increase in the effective magnetization discovered in our previous work [21] and the high values of the *MR* in the case of the films grown at 300 and 400°C.

It can be seen from Fig. 4 that the magnitude of the *MR* of the film grown on the thick layer of SiO_2 (curve (*d*)) increases to 0.9% at an increase in the applied external field to ~0.4 T. This value of the *MR* is close to those obtained for the polycrystalline films of Fe_3O_4 grown on a kapton substrate and glass (increase by 1–1.5% with an increase in the field to 0.4–0.63 T) [12, 17, 30]. On the other hand, it can be seen from the figure that the values of the *MR* for this magnetite film are several times greater than the values for the magnetite film grown on an ultrathin SiO_2 layer at 300°C (curve (*b*)). We connect this significant difference with the fact that, in the case of the ultrathin layer of SiO_2, the electric current flows not only through the Fe_3O_4 film, but also through the Si substrate. Thus, our recent investigation [31] of the electrical conductivity of the Fe_3O_4 film grown on a 5-nm SiO_2/Si(001) layer showed that, at room temperature there is a second channel of conductivity through the Si(001) substrate due to the thermionic emission of electrons into it.

4. CONCLUSIONS

Polycrystalline films of magnetite on the surface of Si(001) substrates coated with an ultrathin layer of SiO_2 have been grown by the method of the reactive deposition of Fe in an O_2 atmosphere. A comparative analysis of the experimental data obtained by the meth-

ods of transmission electron microscopy (TEM) and reflection high-energy electron diffraction (RHEED) has been performed. In contrast to TEM, the data obtained by the RHEED method have shown the presence in the film of magnetite of a texture, the axis of which was normal to the SiO_2/Si(001) surface. It has been revealed that the films grown at a low temperature contain grains with a (100) orientation. With an increase in the growth temperature of 200–400°C, the volume fraction of grains with the preferred (311) orientation increases, while that with the (100) orientation decreases. The angular deviation $\Delta\phi$ of the direction [311] from the axis of the texture is equal to ~15° and is independent of the temperature of the synthesis of the films.

The study of the conductivity of the Fe_3O_4 films as a function of the value of the applied external magnetic field has shown that an increase in the temperature of synthesis leads to an increase in the magnetoresistance.

ACKNOWLEDGMENTS

This work was supported in part by the "Far East" program of the Russian Academy of Sciences, no. 0262-2015-0057.

REFERENCES

1. Z. Zhang and S. Satpathy, "Electron states, magnetism, and the Verwey transition in magnetite", Phys. Rev. B: Condens. Matter **44**, 13319–13331 (1991).
2. I. Zutic, J. Fabian, and S. das Sarma, "Spintronics: Fundamentals and applications", Rev. Modern Phys. **76**, 323–332 (2004).
3. T. Suzuki, T. Sasaki, T. Oikawa, M. Shirashi, Y. Suzuki, and K. Noguchi, "Room-temperature electron spin transport in a highly doped Si channel", Appl. Phys. Express **4**, 023003 (2011).
4. T. Fujii, M. Takano, R. Katano, Y. Bando, and Y. Isozumi, "Preparation and characterization of (111)-oriented Fe_3O_4 films deposited on sapphire", J. Appl. Phys. **66**, 3168–3172 (1989).
5. A. V. Ramos, J.-B. Moussy, M.-J. Guittet, A. M. Bataille, M. Gautier-Soyer, M. Viret, C. Gatel, P. Bayle-Guillemaud, and E. Snoeck, "Magnetotransport properties of Fe_3O_4 epitaxial thin films: Thickness effects driven by antiphase boundaries", J. Appl. Phys. **100**, 103902 (2006).
6. Y. X. Lu, J. S. Claydon, Y. B. Xu, S. M. Thompson, K. Wilson, and G. van der Laan, "Epitaxial growth and magnetic properties of half-metallic Fe_3O_4 on GaAs(100)", Phys. Rev. B: Condens. Matter Mater. Phys. **70**, 233304 (2004).
7. T. Kado, "Structural and magnetic properties of magnetite-containing epitaxial iron oxide films grown on MgO(001) substrates", J. Appl. Phys. **103**, 043902 (2008).
8. S. Tiwari, R. Prakash, R. J. Choudhary, and D. M. Phase, "Oriented growth of Fe_3O_4 thin film on crystalline and amorphous substrates by pulsed laser deposition", J. Phys. D: Appl. Phys. **40**, 4943–4947 (2007).
9. R. J. Kennedy and P. A. Stamp, "Fe_3O_4 films grown by laser ablation on Si(100) and GaAs(100) substrates with and without MgO buffer layers", J. Phys. D: Appl. Phys. **32**, 16–21 (1999).
10. M. L. Parames, J. Mariano, Z. Viskadourakis, N. Popovici, M. S. Rogalski, J. Giapintzakis, and O. Conde, "PLD of Fe_3O_4 films: Influence of background gas on surface morphology and magnetic properties", Appl. Surf. Sci. **252**, 4610–4614 (2006).
11. Y. K. Kim and M. Oliveria, "Magnetic properties of reactively sputtered $Fe_{1-x}O$ and Fe_3O_4 thin films", J. Appl. Phys. **75**, 431–437 (1994).
12. W. B. Mi, H. Liu, Z. Q. Li, P. Wu, E. Y. Jiang, and H. L. Bai, "Evolution of structure, magnetic and transport properties of sputtered films from Fe to Fe_3O_4", J. Phys. D: Appl. Phys. **39**, 5109–5115 (2006).
13. C. Park, Y. Peng, J.-G. Zhu, D. E. Laughlin, and R. M. White, "Magnetoresistance of polycrystalline Fe_3O_4 films prepared by reactive sputtering at room temperature", J. Appl. Phys. **97**, 10C303 (2005).
14. J. Tang, K.-Y. Wang, and W. Zhou, "Magnetic properties of nanocrystalline Fe_3O_4 films", J. Appl. Phys. **89**, 7690–7692 (2001).
15. S. Tiwari, R. J. Choudhary, R. Prakash, and D. M. Phase, "Growth and properties of pulsed laser deposited thin films of Fe_3O_4 on Si substrates of different orientation", J. Phys.: Condens. Matter **19**, 176002 (2007).
16. C. Boothman, A. M. Sanchez, and S. van Dijken, "Structural, magnetic, and transport properties of Fe_3O_4/Si(111) and Fe_3O_4/Si(001)", J. Appl. Phys. **101**, 123903 (2007).
17. G. Zhang, C. Fan, L. Pan, F. Wang, P. Wu, H. Qiu, Y. Gu, and Y. Zhang, "Magnetic and transport properties of magnetite thin films", J. Magn. Magn. Mater. **293**, 737–745 (2005).
18. S. Jain, A. O. Adeyeye, and C. B. Boothroyd, "Electronic properties of half-metallic Fe_3O_4 films", J. Appl. Phys. **97**, 093713 (2005).
19. X. Huang and J. Ding, "The structure, magnetic and transport properties of Fe_3O_4 thin films on different substrates by pulsed laser deposition", J. Korean Phys. Soc. **62**, 2228–2232 (2013).
20. V. V. Balashev, V. A. Vikulov, T. A. Pisarenko, and V. V. Korobtsov, "Effect of oxygen pressure on the texture of a magnetite film grown by reactive deposition on a SiO_2/Si(100) surface", Phys. Solid State **57**, 2532–2536 (2015).
21. V. A. Vikulov, V. V. Balashev, T. A. Pisarenko, A. A. Dimitriev, and V. V. Korobtsov, "The effect of synthesis temperature on structural and magnetic properties of Fe_3O_4 Films Grown on the SiO_2/Si(001) surface", Tech. Phys. Lett. **38**, 336–339 (2012).
22. A. Ishizaka and Y. Shiraki, "Low temperature surface cleaning of silicon and its application to silicon MBE", J. Electrochem. Soc. **133**, 666–671 (1986).
23. H. A. Kobayashi, O. Maida, M. Takahashi, and H. Iwasa, "Nitric acid oxidation of Si to form ultrathin silicon dioxide layers with a low leakage current density", J. Appl. Phys. **94**, 7328–7335 (2003).

24. I. Petrov, P. B. Barna, L. Hultman, and J. E. Greene, "Microstructural evolution during film growth", J. Vac. Sci. Technol. A **21**, S117–S128 (2003).

25. R. D. Heidenreich, *Fundamentals of Transmission Electron Microscopy* (Interscience Publishers, New York, 1964).

26. V. V. Balashev, V. V. Korobtsov, T. A. Pisarenko, and L. A. Chebotkevich, "Growth of Fe_3O_4 films on the Si(111) surface covered by a thin SiO_2 layer", Tech. Phys. Lett. **56**, 1501–1507 (2011).

27. J. T. Drotar, T.-M. Lu, and G.-C. Wang, "Real-time observation of initial stages of copper film growth on silicon oxide using reflection high-energy electron diffraction", J. Appl. Phys. **96**, 7071–7079 (2004).

28. M. Zies, R. Höhne, H. C. Semmelhack, H. Reckentin, M. H. Hong, and P. Esquinazi, "Mechanism of grain-boundary magnetoresistance in Fe_3O_4 films", Eur. Phys. J. B **28**, 415–422 (2002).

29. H. Liu, E. Y. Jiang, and H. L. Bai, "Structures and transport properties of polycrystalline Fe_3O_4 films", J. Phys.: Condens. Matter **15**, 8003–8009 (2003).

30. H. Liu, E. Y. Jiang, H. L. Bai, R. K. Zheng, and X. X. Zhang, "Thickness dependence of magnetic and magneto-transport properties of polycrystalline Fe_3O_4 films prepared by reactive sputtering at room temperature", J. Phys. D: Appl. Phys. **36**, 2950–2953 (2003).

31. V. A. Vikulov, A. A. Dimitriev, V. V. Balashev, T. A. Pisarenko, and V. V. Korobtsov, "Low-temperature conducting channel switching in hybrid Fe_3O_4/SiO2/*n*-Si structures", Mat. Sci. Eng., B **211**, 33–36 (2016).

Translated by S. Gorin